NANO LETTERS

2001
Vol. 1, No. 3
149−153

Nanostructure Processing of Hydroxyapatite-based Bioceramics

Edward S. Ahn, Nathaniel J. Gleason, Atsushi Nakahira, and Jackie Y. Ying*

Department of Chemical Engineering, Massachusetts Institute of Technology, Cambridge, Massachusetts 02139-4307

Received December 6, 2000

Downloaded by NAT LIB UKRAINE on August 5, 2009
Published on February 27, 2001 on http://pubs.acs.org | doi: 10.1021/nl0055299

ABSTRACT

Nanostructure processing was applied to derive hydroxyapatite and hydroxyapatite-zirconia bioceramics with ultrafine microstructures and significantly improved mechanical properties for orthopedic and dental implant applications. Despite its attractive bioactivity, hydroxyapatite (HAP) has been limited in applications due to the poor processability and mechanical strength of the conventional material. Through nanostructure processing, high-strength HAP has been obtained by pressure-assisted sintering. To further toughen the HAP matrix, nanocrystalline yttria-stabilized zirconia (YSZ) dispersoids have been introduced during HAP precipitation. The nanostructured HAP and HAP–YSZ composites demonstrated excellent chemical and microstructural uniformity and mechanical properties, compared to conventional coarse-grained systems.

In the past decade, significant research efforts have been devoted to nanostructure processing as a means to achieve materials with ultrafine microstructures for structural, catalytic, electronic, and optical applications.[1−5] Metallic, intermetallic, and ceramic nanocrystals have been consolidated to form nanostructured materials that have mechanical properties substantially different from their conventional coarse-grained counterparts.[6−8] Nanostructure processing improves the sinterability of ceramics and enhances the mechanical reliability by reducing flaw sizes. The high volume fraction of grain boundaries in nanocrystalline ceramic compacts also provides for increased ductility and superplasticity for low-temperature net-shape forming.[7] Although the high surface reactivity associated with nanocrystalline materials has been exploited for catalytic applications,[9−13] few researchers have considered the biomedical applications of nanostructured materials. Recent studies have reported that nanocrystalline alumina possesses bioactivity, whereas alumina is bioinert in the conventional polycrystalline form.[14−15]

In this study, we are interested in developing nanocrystalline bioceramics, such as hydroxyapatite (HAP), that have excellent bioactivity. HAP is a bioactive ceramic with a crystal structure similar to native bone and teeth minerals. It has generated great interest as an advanced orthopedic and dental implant candidate because it elicits a favorable biological response and forms a bond with the surrounding tissues.[16] However, applications of HAP are currently limited to powders, coatings, porous bodies, and nonload-bearing implants due to processing difficulties and the poor mechanical properties of conventional HAP.[17] This material is sensitive to nonstoichiometry and impurities due to its complex composition and crystal structure ($Ca_{10}(PO_4)_6(OH)_2$, $P6_3/m$).[18−19] As a result, conventionally processed HAP materials lack phase purity and homogeneity. They are very challenging to sinter; densification has typically required high temperatures, which result in grain growth and decomposition into undesired phases with poor mechanical and chemical stability.[20−21] To circumvent densification at high temperatures, glassy additives can be introduced to promote liquid-phase sintering at a lower temperature. However, the presence of a secondary glassy phase gives rise to poor mechanical characteristics.[22]

In this research, nanostructure processing is successfully applied to HAP to achieve superior chemical homogeneity and microstructural uniformity, so that high-quality apatite-based bioceramics can be generated at low sintering temperatures. We have also examined nanostructure processing as a means to create composites with controlled mixing of components. This concept is used to introduce highly dispersed yttria-stabilized zirconia (YSZ) nanocrystals to structurally reinforce the HAP matrix. By achieving a nanocomposite of HAP−YSZ with a controlled microstructure, we can further improve the mechanical properties of HAP-based bioceramics for important load-bearing implant applications.

Previous research on nanocrystalline ceramics has focused mainly on simple oxides and nitrides.[2,7,8,23−24] To successfully process a complex system such as HAP, we have chosen the chemical precipitation approach because this wet-

* To whom correspondence should be addressed. Tel: +1-617-253-2899. Fax: +1-617-258-5766. E-mail: jyying@mit.edu.

10.1021/nl0055299 CCC: $20.00 © 2001 American Chemical Society
Published on Web 02/27/2001

chemical route[20,25] will likely generate the desired stoichiometry, crystalline phase and grain size at low temperatures. To precipitate HAP, 0.167 M $Ca(NO_3)_2 \cdot 4H_2O$ was slowly added (1.5 mL/min) to 0.1 M $(NH_4)_2HPO_4$ at the specified aging temperature in our preliminary studies to control the crystallization of HAP and to prevent the formation of undesirable secondary phases. The pH's of these precursor solutions were adjusted by the addition of concentrated NH_4OH. After aging, the white precipitate was washed, dried, and calcined at 550 °C in flowing oxygen. We have examined synthesis parameters such as precursor pH, aging time, and temperature to achieve HAP particles with tailored composition, crystallite size, morphology, and surface chemistry to optimize their chemical stability, sinterability, and mechanical properties.

The pH of the starting solutions can affect chemical precipitation by altering the solubility of the system and by affecting powder agglomeration. As the pH was increased, a preferred growth along the ⟨002⟩ axis of HAP was observed in X-ray diffraction (XRD) patterns, resulting in an increasingly rodlike morphology and a larger average particle size. The precipitate produced with $Ca(NO_3)_2 \cdot 4H_2O$ and $(NH_4)_2HPO_4$ precursor solutions of matching pH (10.4) gave rise to stoichiometric HAP powders that sintered to 98.5% theoretical density. In contrast, samples that were produced at a higher ($Ca(NO_3)_2 \cdot 4H_2O$ solution pH = 11.8 and $(NH_4)_2HPO_4$ solution pH = 11) or lower pH ($Ca(NO_3)_2 \cdot 4H_2O$ solution pH = 6.1 and $(NH_4)_2HPO_4$ solution pH = 10.4) resulted in nonstoichiometric HAP that underwent phase decomposition during sintering.

We have found that aging was critical toward obtaining well-crystallized HAP particles with uniform morphologies. Occluded impurities are removed and crystal strain is reduced in the aging process, whereas grains with nonuniform morphologies redissolve and are re-crystallized into more ordered forms. Longer aging times also ensure that the reagents are fully reacted and precipitated. It was noted that an aging period of 100 h led to small crystallite sizes (~50 nm as verified by transmission electron microscopy (TEM) and XRD peak broadening analysis) and high surface areas (~90 m^2/g) for the 550 °C-calcined HAP powder. This sample was sintered easily without phase decomposition. In contrast, the sample that was not subjected to aging underwent severe decomposition upon sintering, indicating that the as-precipitated phase was not thermally stable due to its poor compositional uniformity.

Varying the aging temperature also influences the crystal growth and chemistry. The sample aged at 0 °C was highly nonstoichiometric (Ca/P = 1.44 instead of 1.67), and decomposed into coarse-grained β-tricalcium phosphate during sintering. In contrast, aging at 25 °C produced a stoichiometric powder with a spherical morphology, which can be easily densified to produce a nanostructured, phase-pure HAP compact. A higher aging temperature of 80 °C led to whiskerlike HAP particles with a preferential growth along the ⟨002⟩ axis (200 nm). When this sample was sintered, a pellet with grains and pores on the order of 100 nm was obtained.

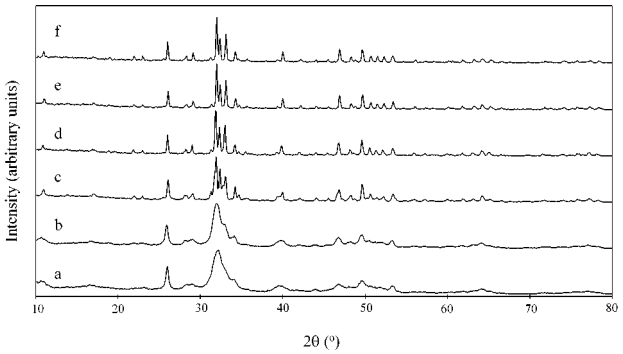

Figure 1. XRD patterns (Siemens D5000 diffractometer, 45 kV, 40 mA, Cu K_α) of nanocrystalline HAP (a) as-synthesized, (b) after 550 °C calcination in oxygen, and after pressureless sintering in oxygen at (c) 1000 °C, (d) 1100 °C, (e) 1200 °C, and (f) 1300 °C. All peaks correspond to hydroxyapatite.

Stoichiometric, equiaxed, nanocrystalline HAP powders demonstrated significantly enhanced sinterability. The optimized system could be fully densified by pressureless sintering at 1000 °C for 2 h, in contrast to 1100 °C that was required for the best HAP system reported in the literature.[20,25−26] In comparison, commercial HAP (Aldrich) powders could not be sintered to >70% theoretical density via pressureless sintering. XRD studies indicated that the nanocrystalline HAP materials produced were thermally stable up to 1300 °C, whereas commercial HAP materials underwent decomposition to β-tricalcium phosphate by 1000 °C. The decomposition reaction, $Ca_{10}(PO_4)_6(OH)_2 \rightarrow 3Ca_3(PO_4)_2 + CaO + H_2O$, has been found to be promoted by the presence of minute impurities or nonstoichiometry in the HAP powders.[27] The excellent compositional homogeneity and phase purity associated with our nanocrystalline HAP samples stabilized them against decomposition at high temperatures, so that dense specimens with superior mechanical integrity could be achieved without the undesired phases, as demonstrated in Figure 1.

Full densification of the optimized HAP powders could also be achieved in 30 min at a remarkably low temperature of 900 °C with pressure-assisted sintering (load = 100 MPa). The large number of pores in Figure 2a shows that the compacts produced from commercial HAP powders were not sintered under such conditions. Scanning electron microscopy (SEM) at a higher magnification revealed the presence of large β-tricalcium phosphate ($Ca_3(PO_4)_2$) and calcia (CaO) grains associated with decomposition reactions (Figure 2b), as revealed by XRD. These decomposition reactions may be the major barrier in the densification of commercial HAP. In contrast, nanocrystalline HAP was fully densified without phase decomposition (Figure 2c) and possessed an ultrafine microstructure (Figure 2d). High-resolution TEM images illustrate that the sintered compact possessed a uniform and ultrafine microstructure with an average grain size of ~100 nm (Figure 3a), with no glassy or amorphous interfaces along the grain boundaries (Figure 3b). The crystallinity of the HAP grains and the grain boundaries suggests that the material has excellent phase homogeneity and purity. These microstructural features could be credited for the superior strength of nanostructured HAP compared to conventional HAP,

Downloaded by NAT LIB UKRAINE on August 5, 2009
Published on February 27, 2001 on http://pubs.acs.org | doi: 10.1021/nl0055299

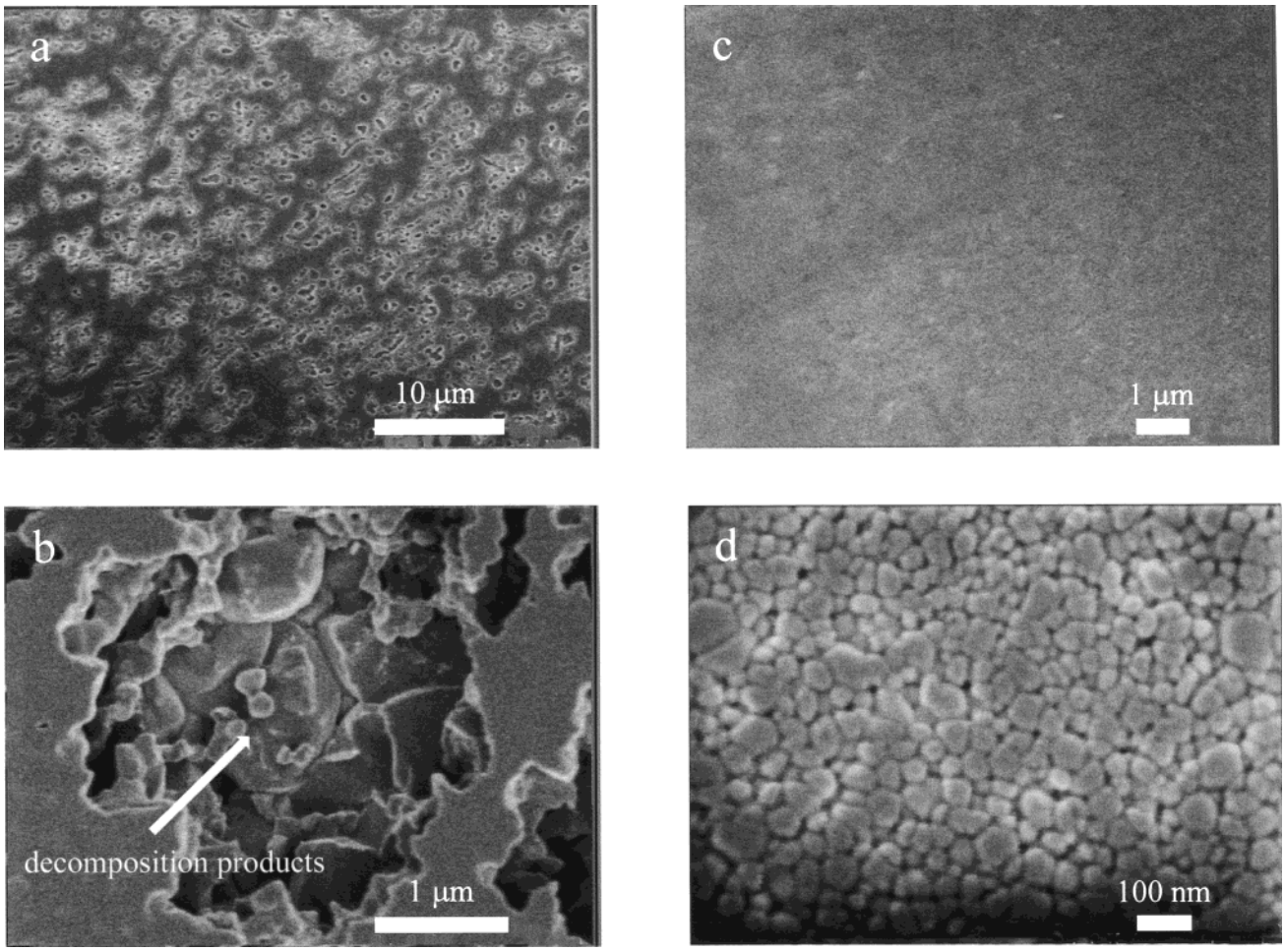

Figure 2. (a,b) SEM micrographs (JEOL 6320 Field Emission Gun Scanning Electron Microscope) of polished cross-sections of commercial HAP pressure-assisted sintered at 900 °C, showing (a) a porous microstructure and (b) β-tricalcium phosphate and calcia decomposition products. (c,d) SEM micrographs of polished cross-sections of nanocrystalline HAP pressure-assisted sintered at 900 °C, showing (c) a dense, uniform microstructure composed of (d) ultrafine grains.

Downloaded by NAT LIB UKRAINE on August 5, 2009
Published on February 27, 2001 on http://pubs.acs.org | doi: 10.1021/nl0055299

Table 1. Mechanical Properties of Nanostructured HAP Compared to Conventional HAP, Dental Enamel, and Compact Bone

	compressive strength (MPa)	bending strength (MPa)	fracture toughness (MPa·m$^{1/2}$)[b]
nanostructured HAP[a]	879	193	1.3[§]
conventional HAP[c,a]	120−800	38−113	1.0
dental enamel[d]	95−370	76	
compact bone[d]	170−193	160	2−12

[a] Prepared by pressure-assisted sintering. [b] Fracture toughness was evaluated using a Vickers indentation method.[29,30] [c] Refs 17,20,21, and 31. [d] Ref 17.

dental enamel, and compact bone. Table 1 shows that the nanostructured HAP compact has superb compressive strength. Although conventional HAP has a lower bending strength than compact bone, nanostructured HAP demonstrated a greater bending strength than compact bone and dental enamel, indicating that this new material would be suitable as an orthopedic and dental implant material. Our study also showed that nanostructured HAP has a greater fracture toughness than conventional HAP, but the value is still lower than that of compact bone.

To improve the fracture resistance of our bioceramics against crack initiation and propagation, we have introduced 3 mol % yttria-stabilized zirconia (YSZ) to nanostructured HAP to form a HAP−YSZ nanocomposite system containing 3 wt % YSZ. The YSZ dispersoids can mechanically reinforce the HAP matrix through crack deflection and phase transformation toughening. Previous researchers have found that HAP−YSZ composites are extremely difficult to densify, requiring pressure-assisted sintering at 1400 °C followed by hot isostatic pressing,[28,29] resulting in significant HAP decomposition and grain growth.[29] Conventional composites also utilize large amounts of YSZ (a bioinert ceramic) in structural reinforcement, thereby inhibiting bioactivity. Our goal is to attain a high YSZ dispersion in the HAP matrix to circumvent the need for high YSZ loading in structural toughening. The low YSZ content would also ensure excellent in vivo interactions, while matching closely the mechanical properties of natural bone. To achieve these design objectives, we have prepared a HAP−YSZ nanocomposite by a colloidal addition technique, which allows for the manipulation of composite microstructure on the nanometer scale. In our synthesis, YSZ was chemically precipitated by slowly adding a 0.2 M $ZrOCl_2 \cdot 8H_2O$ with 3

Downloaded by NAT LIB UKRAINE on August 5, 2009
Published on February 27, 2001 on http://pubs.acs.org | doi: 10.1021/nl0055299

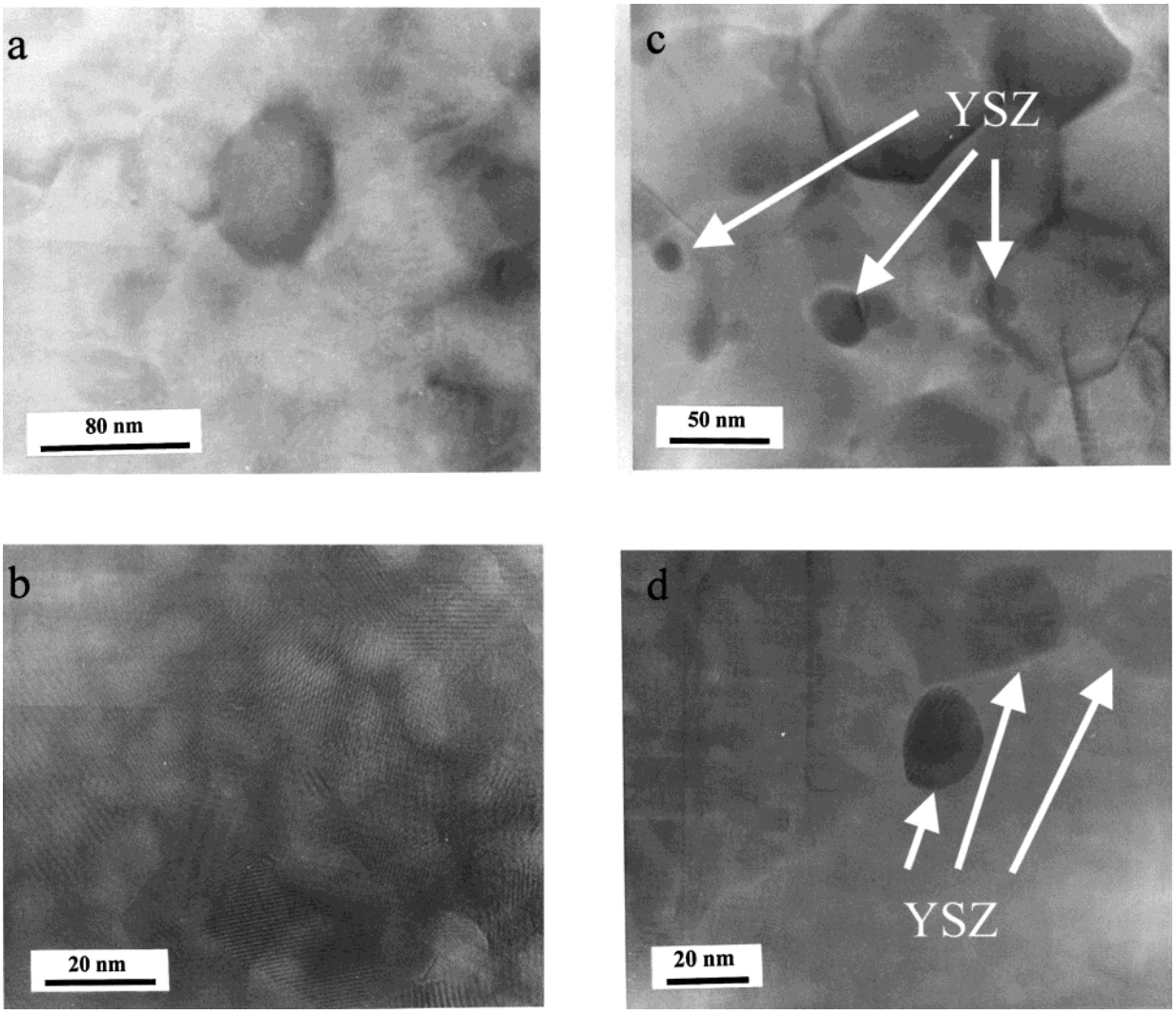

Figure 3. Thin-section TEM micrographs (JEOL 2010, 200 kV) of (a,b) a nanostructured HAP compact that has been subjected to pressure-assisted sintering at 900 °C, and (c,d) a HAP−YSZ nanocomposite compact (with 3 wt % YSZ) that has been subjected to pressure-assisted sintering at 1000 °C.

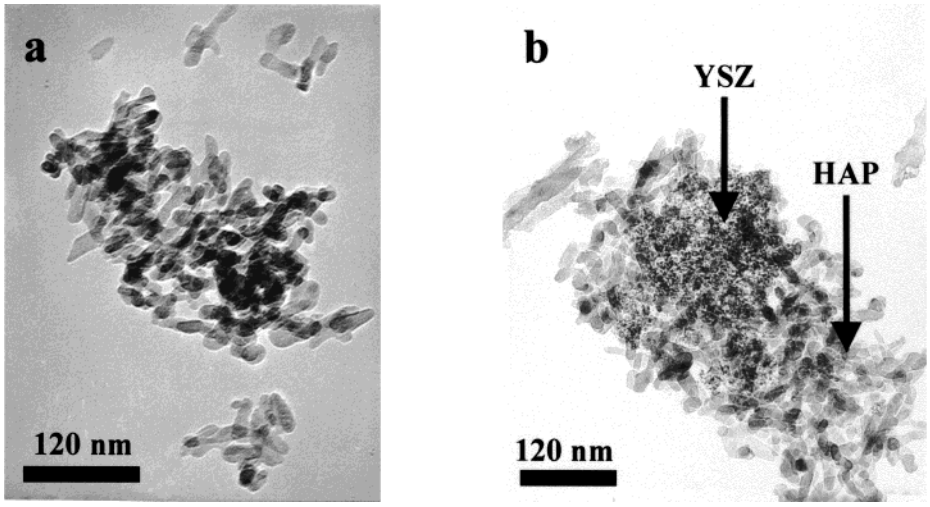

Figure 4. TEM micrographs (JEOL 2000, 200 kV) of (a) nanocrystalline HAP powders prepared by chemical precipitation, and (b) HAP−YSZ nanocomposite powders (with 3 wt % YSZ) prepared by the colloidal addition technique.

mol % $Y(NO_3)_3 \cdot 4H_2O$ ethanolic solution to a NH_4OH-ethanol solution. The resulting sol was aged under hydrothermal conditions at 120 °C for 12 h. $(NH_4)_2HPO_4$ and $Ca(NO_3)_2 \cdot 4H_2O$ were then added to the YSZ sol for

precipitation at a matched pH of 10.4. TEM micrographs show that the structure and morphology of the HAP nanocrystals (Figure 4a) remained unaltered upon the incorporation of YSZ nanocrystals (see Figure 4b). Furthermore, Figure 4b illustrates that the colloidal addition technique resulted in an intimate mixing of the two components.

We have successfully obtained highly dispersed YSZ grains in a dense HAP matrix (Figure 3c); the nanocomposite powders were densified via pressure-assisted sintering by 1000 °C (load = 50 MPa). High-resolution TEM (Figure 3d) shows that the interfaces between HAP and YSZ grains are highly crystalline in nature. Because potential cracks would likely propagate along the grain boundaries in materials with such an ultrafine microstructure, the high intergranular dispersion of YSZ nanocrystals by the colloidal addition technique would be very beneficial. It would provide an excellent degree of interaction between YSZ grains and the HAP matrix, uniformly enhancing the toughness of the system. Indeed, we have found that with only 3 wt % YSZ addition, the fracture toughness of a HAP-based nanocomposite could be increased significantly to 2.0 MPa·$m^{1/2}$, which was comparable to that of compact bone.

This study shows that nanostructure processing offers attractive solutions to challenges encountered in HAP processing. Particle size and morphology, stoichiometry, and phase homogeneity and purity can be controlled to provide HAP with significantly enhanced sinterability and stability. Fully dense, transparent HAP compacts have been successfully achieved at temperatures as low as 900 °C, while retaining the ultrafine microstructure. The nanostructured HAP results in a 70% improvement over the best conventional HAP in the critical 3-point bending strength. The versatility of nanostructure processing was further demonstrated in the production of HAP−YSZ nanocomposites. An ultrahigh dispersion of YSZ was achieved so that a low loading of 3 wt % YSZ was sufficient to effectively increase the fracture toughness of HAP to closely match that of compact bone. This approach brings about improved mechanical properties without sacrificing biocompatibility, so that the resulting HAP-based systems hold wide potential applicability as load-bearing implants, bone grafts, and dental replacements.

Downloaded by NAT LIB UKRAINE on August 5, 2009
Published on February 27, 2001 on http://pubs.acs.org | doi: 10.1021/nl0055299

Acknowledgment. This work was supported by the David and Lucile Packard Foundation and the Office of Naval Research (N00014-95-1-0626)

References

(1) Gleiter, H. *Prog. Mater. Sci.* **1989**, *33*, 233.
(2) Siegel, R. W. *Annu. Rev. Mater. Sci.* **1991**, *21*, 559.
(3) Dag, O.; Kuperman, A.; Ozin, G. A. *Adv. Mater.* **1995**, *7*, 72.
(4) Ying, J. Y.; Sun, T. *J. Electroceram.* **1997**, *1*, 219.
(5) Ying, J. Y. *AIChE J.* **2000**, *46*, 1902.
(6) Padamanabhan, K. A.; Hahn, H. In *Synthesis and Processing of Nanocrystalline Powders*; Bourell, D. L., Ed.; The Mineral, Metals and Materials Society: Philadelphia, PA, 1996.
(7) Mayo, M. J. In *Nanostructured Materials: Science and Technology*; Chow, G.-M., Noskova, N. I., Eds.; Kluwer: Netherlands, 1998.
(8) Niihara, K. *J. Ceram. Soc. Jpn.* **1991**, *99*, 974.
(9) Tschöpe, A.; Liu, W.; Flytzani-Stephanopoulos, M.; Ying, J. Y. *J. Catal.* **1995**, *157*, 42.
(10) Fokema, M. D.; Ying, J. Y. *Appl. Catal. B: Environ.* **1998**, *18*, 71.
(11) Zhang, Z.; Wang, C.-C.; Zakaria, R.; Ying, J. Y. *J. Phys. Chem. B.* **1998**, *102*, 10871.
(12) Mehnert, C. P.; Weaver, D. W.; Ying, J. Y. *J. Am. Chem. Soc.* **1998**, *120*, 12 289.
(13) Zarur, A. J.; Ying, J. Y. *Nature* **2000**, *403*, 65.
(14) Webster, T. J.; Siegel, R. W.; Bizios, R. In *Bioceramics*; LeGeros, R. Z., LeGeros, J. P., Eds.; World Scientific Publishing: New York, 1998; Vol. 11.
(15) Webster, T. J.; Siegel, R. W.; Bizios, R. *Biomater.* **1999**, *20*, 1221.
(16) Hench, L. L. *J. Am. Ceram. Soc.* **1991**, *74*, 1487.
(17) Suchanek, W.; Yoshimura, M. *J. Mater. Res.* **1998**, *13*, 94.
(18) Slosarczyk, A.; Stobierska, E.; Pazkiewicz, Z.; Gawlicki, M. *J. Am. Ceram. Soc.* **1996**, *79*, 2539.
(19) Fulmer, M. T.; Martin, R. I.; Brown, P. W. *J. Mater. Sci. Mater. Med.* **1992**, *79*, 2539.
(20) Akao, M.; Aoki, H.; Kato, K. *J. Mater. Sci.* **1981**, *16*, 809.
(21) Ruys, A. J.; Wei, M.; Sorrell, C. C.; Dickson, M. R.; Brandwood, A.; Milthorpe, B. K. *Biomater.* **1995**, *16*, 409.
(22) Santos, J. D.; Knowles, J. C.; Reis, R. L.; Monteiro, F. J.; Hastings, G. W. *Biomater.* **1994**, *15*, 5.
(23) Panchula, M. L.; Ying, J. Y. In *Nanostructured Materials: Science and Technology*; Chow, G.-M., Noskova, N. I., Eds.; Kluwer: Netherlands, 1998.
(24) Castro, D. T.; Ying, J. Y. *Nanostr. Mater.* **1997**, *9*, 67.
(25) Jarcho, M.; Bolen, C. H.; Thomas, M. B.; Bobick, J.; Kat, J. F.; Doremus, R. H. *J. Mater. Sci.* **1976**, *11*, 2027.
(26) Fang, Y.; Agrawal, D. K.; Roy, D. M.; Roy, R. *Mater. Lett.* **1995**, *23*, 147.
(27) Uematsu, K.; Takagi, M.; Honda, T.; Uchida, N.; Saito, K. *J. Am. Ceram. Soc.* **1989**, *72*, 1476.
(28) Li, J.; Fartash, B.; Hermansson, L. *Biomater.* **1998**, *16*, 94.
(29) Ioku, K.; Yoshimura, M.; Somiya, S. *Biomater.* **1990**, *11*, 57.
(30) Niihara, K. *Ceram. Jpn.* **1985**, *20*, 12.
(31) With, G. D.; Dijk, H. J. A. V.; Hattu, N.; Prijs, K. *J. Mater. Sci.* **1981**, *16*, 1592.

NL0055299